Supplementary Information

Mechanisms of Hydrogen Evolution by Six-Coordinate Cobalt Complexes: A Density Functional Study on the Role of Redox-Active Pyridinyl-Substituted Diaminotriazine Benzamidine Ligand as a Proton Relay

Kittimeth Thammanatpong[†] and Panida Surawatanawong*[,†,‡]

[†]*Department of Chemistry and Center of Excellence for Innovation in Chemistry, Faculty of Science, Mahidol University, Bangkok 10400, Thailand*

[‡]*Center of Sustainable Energy and Green Materials, Mahidol University, Salaya, Nakhon Pathom 73170, Thailand*

*E-mail: panida.sur@mahidol.ac.th

Table of Contents **Page**

Standard-state conversions[1]

By default, the geometry optimization in Gaussian 16 was carried out at the standard pressure and temperature (1 atm at 298.15 K). To convert to the standard state in the solution phase (1 M at 298.15 K), the equation S1 was applied to convert the free energy from the standard state at 1 atm to the standard state at 1 M. Let A, B, and C as an example of ideal gases,

$$A + B \rightleftharpoons C \quad \text{(S1)}$$

Thus,
$$\Delta G^{\circ\prime} = \Delta G^{\circ} + RTln\frac{Q^{\circ\prime}}{Q^{\circ}} \quad \text{(S2)}$$

where R is the gas constant, T is the temperature, Q is the reaction quotient ($Q = \frac{[B][C]}{[A]}$), Q° is the reaction quotient at 1 atm, $Q^{\circ\prime}$ is the reaction quotient at 1 M, ΔG° is the free energy at 1 atm, and $\Delta G^{\circ\prime}$ is the free energy at 1 M.

The concentration of 1 atm of ideal gas is $\frac{1}{24.46} mol/L$ at 298.15 K.

Thus,
$$\Delta G^{\circ\prime} = \Delta G^{\circ} + RTln\frac{\frac{1\cdot 1}{24.46}}{\frac{1}{24.46\cdot 24.46}} \quad \text{(S3)}$$

$$\Delta G^{\circ\prime} = \Delta G^{\circ} + RTln(24.46) \quad \text{(S4)}$$

Table S1. Calculated reduction potentials (E^0) of $[Co(tpy)_2]^{2+}$ and $[Ru(bpy)_3]^{2+}$.

Reaction	E^0 (V) vs Fc/Fc^+ in CH_3CN	
	Calc[a]	Exp[c]
$^4[Co^{II}(tpy)_2]^{2+} + e^- \rightarrow {}^3[Co^{I}(tpy)_2]^{1+}$	-1.25	-1.19 (-1.17)[d]
$^3[Co^{I}(tpy)_2]^{1+} + e^- \rightarrow {}^4[Co^{II}(tpy^{\bullet -})_2]^{0}$	-2.08	-2.07 (-2.04)[d]
$tpy + e^- \rightarrow tpy^{\bullet -}$	-2.59	-2.52
Reaction	E^0 (V) vs SCE in CH_3CN	
	Calc[b]	Exp[e]
$^1[Ru^{II}(bpy)_3]^{2+} + e^- \rightarrow {}^2[Ru^{I}(bpy)_3]^{1+}$	-1.38	-1.32

[a]The calculated E^0 vs experimental E^0 of ferrocene/ferrocenium (Fc/Fc^+) (4.98 V).[2]
[b]The calculated E^0 vs experimental E^0 (SCE) (4.684 V). This is obtained from E^0 vs E^0 (SHE) (4.44 V),[3] which is converted to E^0 vs E^0 (SCE) (4.684 V) by applying 0.244 V correction.[4]
[c]The experimental E^0 vs Fc/Fc^+ in CH_3CN is from Ferreira et al.[5] The scan rate was 0.05 V/s.
[d]The experimental E^0 vs Fc/Fc^+ in CH_3CN is from Aroua et al.[6]. The scan rate was 0.05 V/s.
[e]The experimental E^0 vs SCE in CH_3CN is from Wacholtz et al.[7] The scan rate was 0.2 V/s.

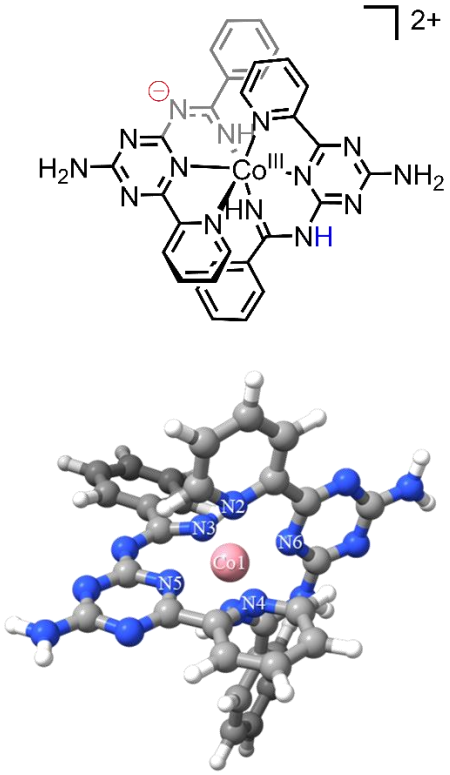

$[Co^{III}(L^{1-})(LH)]^{2+}$

bond distance (Å)	$^1[Co^{III}(L^{1-})(LH)]^{2+}$ X-ray[8]	B3LYP[a]
Co-L^-		
Co-N4(pyridine)	1.962	2.005
Co-N5(triazine)	1.898	1.921
Co-N3(amidinate)	1.887	1.900
Co-LH		
Co-N2(pyridine)	1.973	1.998
Co-N6(triazine)	1.902	1.938
Co-N1(amidine)	1.905	1.925
MUE		0.026

[a]Geometry optimization using B3LYP in DMF solvent with CPCM and the basis set is def2-TZVP for Co and 6-311G(d) for other atoms.

Fig. S1 Selected geometry parameters of the $^1[Co^{III}(L^{1-})(LH)]^{2+}$ (S = 0) from the X-ray crystallography[8] and from the calculation.

Table S2. Calculated reduction potentials for $[Ru(bpy)_3]^{2+}$ and TEOA.

	E^0 (V) vs SCE	
	[a]Calc	[b]Exp
Oxidative quenching		
$^2[Ru^{III}(bpy)_3]^{3+} + e^- \rightarrow {}^*{}^3[Ru^{III}(bpy^{\bullet -})(bpy)_2]^{2+}$	-0.88	-0.81 ± 0.07
Reductive quenching		
$^*{}^3[Ru^{III}(bpy^{\bullet -})(bpy)_2]^{2+} + e^- \rightarrow {}^2[Ru^{II}(bpy^{\bullet -})(bpy)_2]^{1+}$	0.62	0.77 ± 0.07
$TEOA^{\bullet +} + e^- \rightarrow TEOA$	0.63	0.82[c]
$^1[Ru^{II}(bpy)_3]^{2+} + e^- \rightarrow {}^2[Ru^{II}(bpy^{\bullet -})(bpy)_2]^{1+}$	-1.38	-1.33 ± 0.07

[a]The calculated E^0 vs SCE in DMF using B3LYP/BS2 (this work). In BS2, def2-TZVP was used for Co and 6-311++G(d,p) for C, H, N.
[b]The experimental E^0 vs SCE in CH_3CN is from Bock *et al*.[12, 13]
[c]The experimental E^0 vs SCE in aqueous is from Grätzel *et al.*[14]

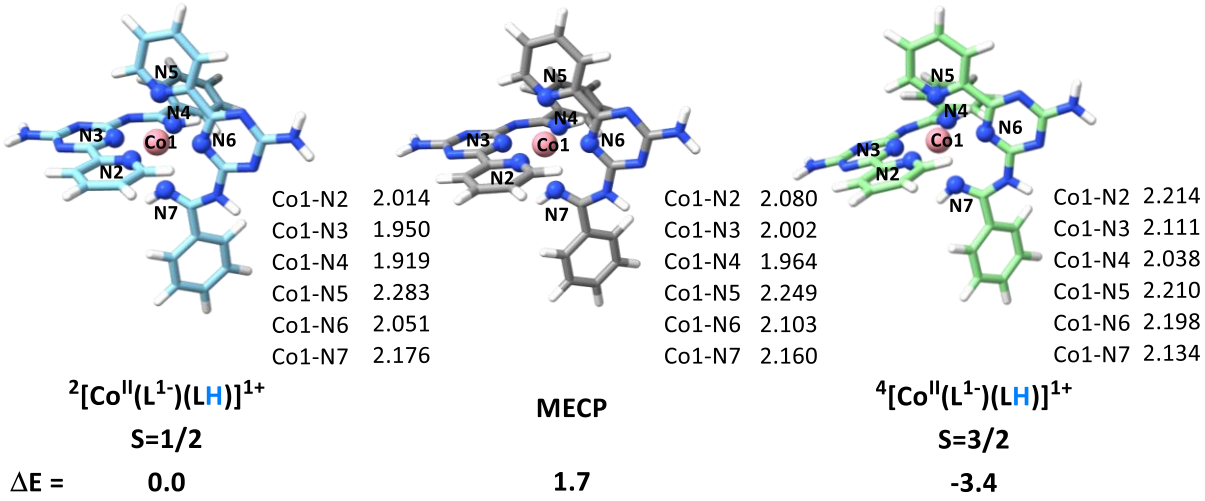

Fig. S2 Optimized geometries and relative electronic energies (ΔE in kcal/mol) for the low spin $^{2}[Co^{II}(L^{1-})(LH)]^{1+}$, minimum energy crossing point (MECP),[15, 16] and the high spin $^{4}[Co^{II}(L^{1-})(LH)]^{1+}$. Selected bond distances are shown in Å.

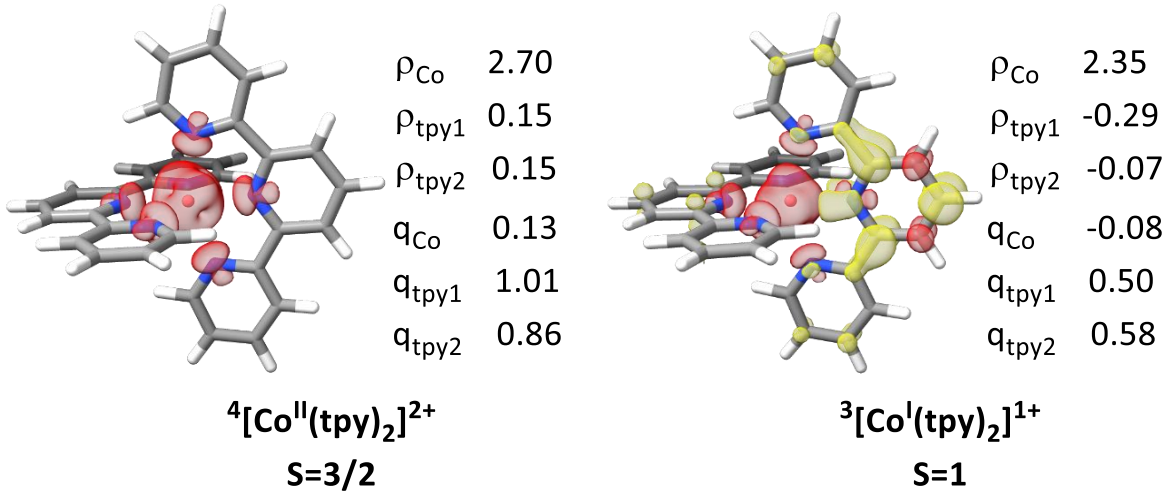

Fig. S3 Spin density plots of $^{4}[Co^{II}(tpy)_2]^{2+}$ and $^{3}[Co^{I}(tpy)_2]^{1+}$. The LÖwdin spin (ρ) and charge population (q) are shown.

Table S3. The solvent corrected relative free energies for intermediates upon reductions of $[Co^{III}(L^{1-})(LH)]^{2+}$ (LH = py-DAT-amidine).

	Spin state		E_{elec} (Hartree)	$<S^2>$	Absolute free energy (Hartree)	Relative free energy (kcal/mol)
$[Co^{III}(L^{1-})(LH)]^{2+}$	**S = 0**		**-3308.034035**	**0.00**	**-3307.560915**	**0.0**
	S = 1		-3307.926622	2.03	-3307.458749	64.1
$[Co^{II}(L^{1-})(LH)]^{1+}$	S = 1/2		-3308.193972	0.76	-3307.730099	6.7
	S = 3/2		**-3308.199443**	**3.76**	**-3307.740761**	**0.0**
$[Co^{II}(L^{1-})(LH^{\bullet 1-})]^{0}$	S = 0	closed shell	-3308.280253	0.00	-3307.816626	27.3
	S = 0	BS(1,1)	-3308.294087	1.02	-3307.832290	17.5
	S = 1	BS(2,0)	-3308.294153	2.02	-3307.848778	7.1
	S = 1	**BS(3,1)**	**-3308.315935**	**3.01**	**-3307.858591**	**0.9**
	S = 2		**-3308.316546**	**6.02**	**-3307.860094**	**0.0**
$[Co^{II}(L^{\bullet 2-})(LH^{\bullet 1-})]^{1-}$	S = 1/2		-3308.412341	1.78	-3307.954403	4.9
	S = 3/2	BS(3,0)	-3308.412613	3.78	-3307.955428	4.2
	S = 3/2	**BS(4,1)**	**-3308.415618**	**4.76**	**-3307.961469**	**0.5**
	S = 5/2		**-3308.416208**	**8.78**	**-3308.043661**	**0.0**
$[Co^{II}(L^{\bullet 2-})(LH^{\bullet\bullet 2-})]^{2-}$	S = 0		-3308.487902	1.02	-3308.033669	9.7
	S = 1		-3308.488198	2.02	-3308.034737	9.1
	S = 2	BS(4,2)	-3308.494776	3.83	-3308.043751	3.4
	S = 2	**BS(5,1)**	**-3308.496390**	**6.89**	**-3308.049177**	**0.0**
	S = 3		-3308.493315	12.04	-3308.043661	3.5

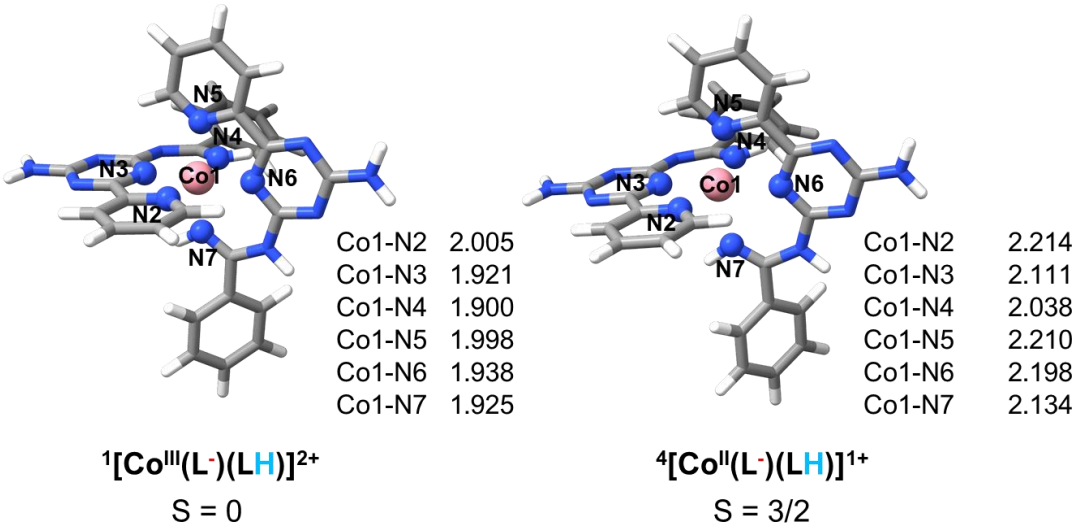

Fig. S4 Optimized geometries of $^{1}[Co^{III}(L^{1-})(LH)]^{2+}$ (S = 0) and $^{4}[Co^{II}(L^{1-})(LH)]^{1+}$ (S = 3/2). Selected bond distances are shown in Å.

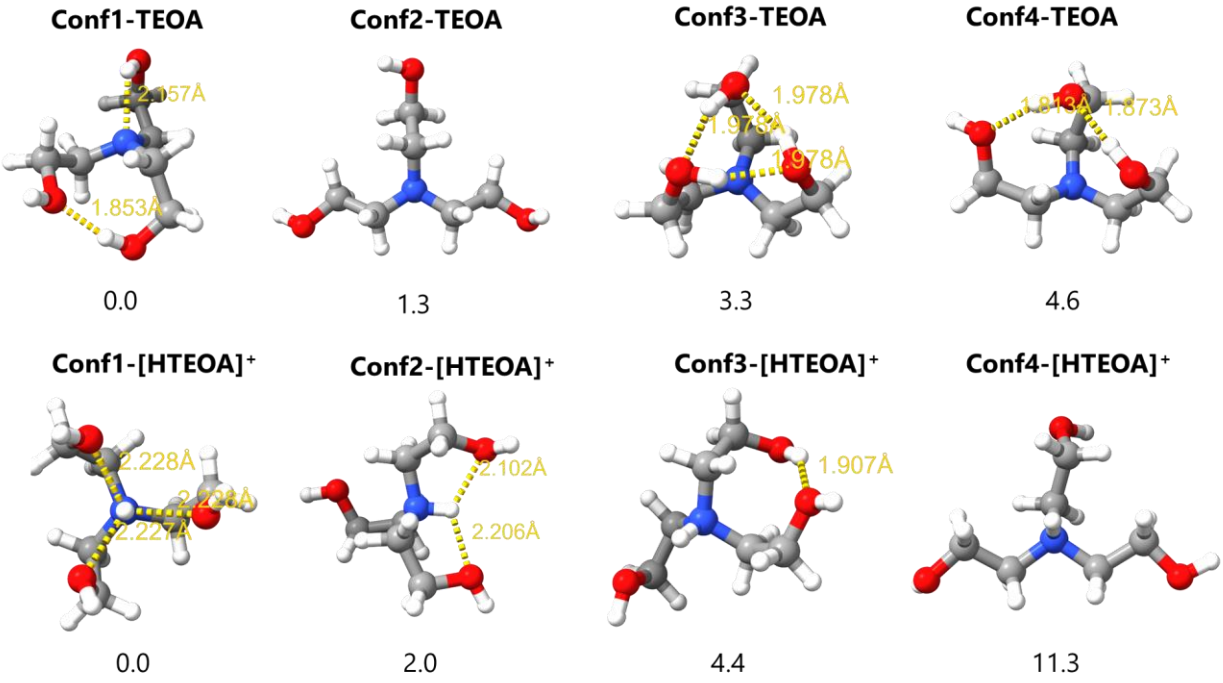

Fig. S5 Optimized geometries of triethanolamine (TEOA) and $[HTEOA]^{+}$. The solvent corrected relative free energies are with respect to the lowest energy conformer (in kcal/mol).

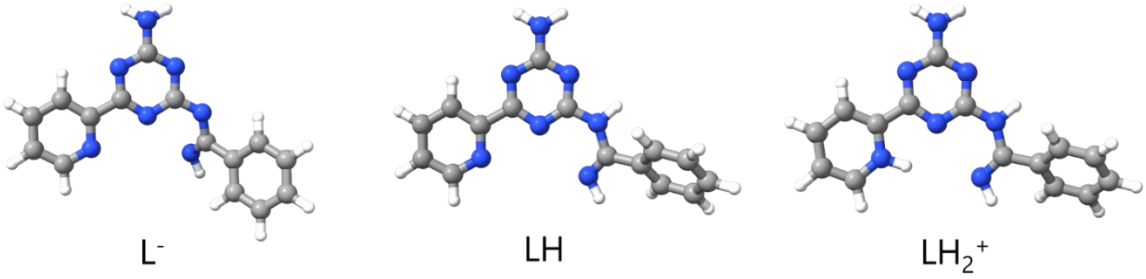

Fig. S6 Optimized geometries of L^-, LH, and LH_2^+.

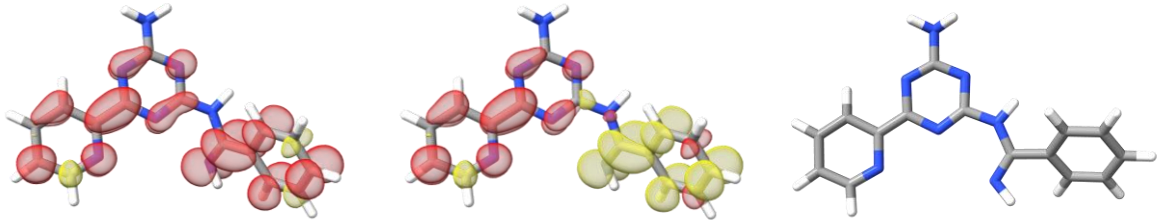

	$LH^{\bullet\bullet 2-}$	$LH^{\bullet\bullet 2-}$	LH^{2-}
	S = 1	S = 0 BS(1,1)	S = 0 Closed-shell singlet
ΔG (kcal/mol)=	0.0	0.6	3.7

Fig. S7 The reduced forms of protonated ligand LH in triplet $LH^{\bullet\bullet 2-}$ (S = 1), open-shell singlet diradical $LH^{\bullet\bullet 2-}$ (S = 0, BS(1,1)) and closed-shell singlet LH^{2-} (S = 0). The solvent corrected relative free energies are with respect to the lowest energy conformer (in kcal/mol).

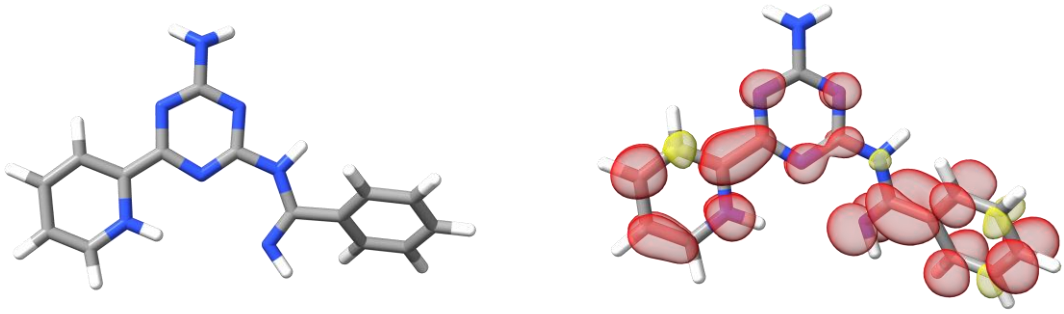

	LH_2^{1-}	$LH_2^{\bullet\bullet 1-}$
	S = 0 Closed-shell singlet	**S = 1**
ΔG (kcal/mol) =	0.0	13.2

Fig. S8 The reduced forms of protonated ligand LH_2 in closed-shell singlet LH_2^{1-} (S = 0) and triplet $LH_2^{\bullet\bullet 1-}$ (S = 1). The open-shell singlet diradical $LH_2^{\bullet\bullet 1-}$ (S = 0, BS(1,1)) was not found. The solvent corrected relative free energies are with respect to the lowest energy conformer (in kcal/mol).

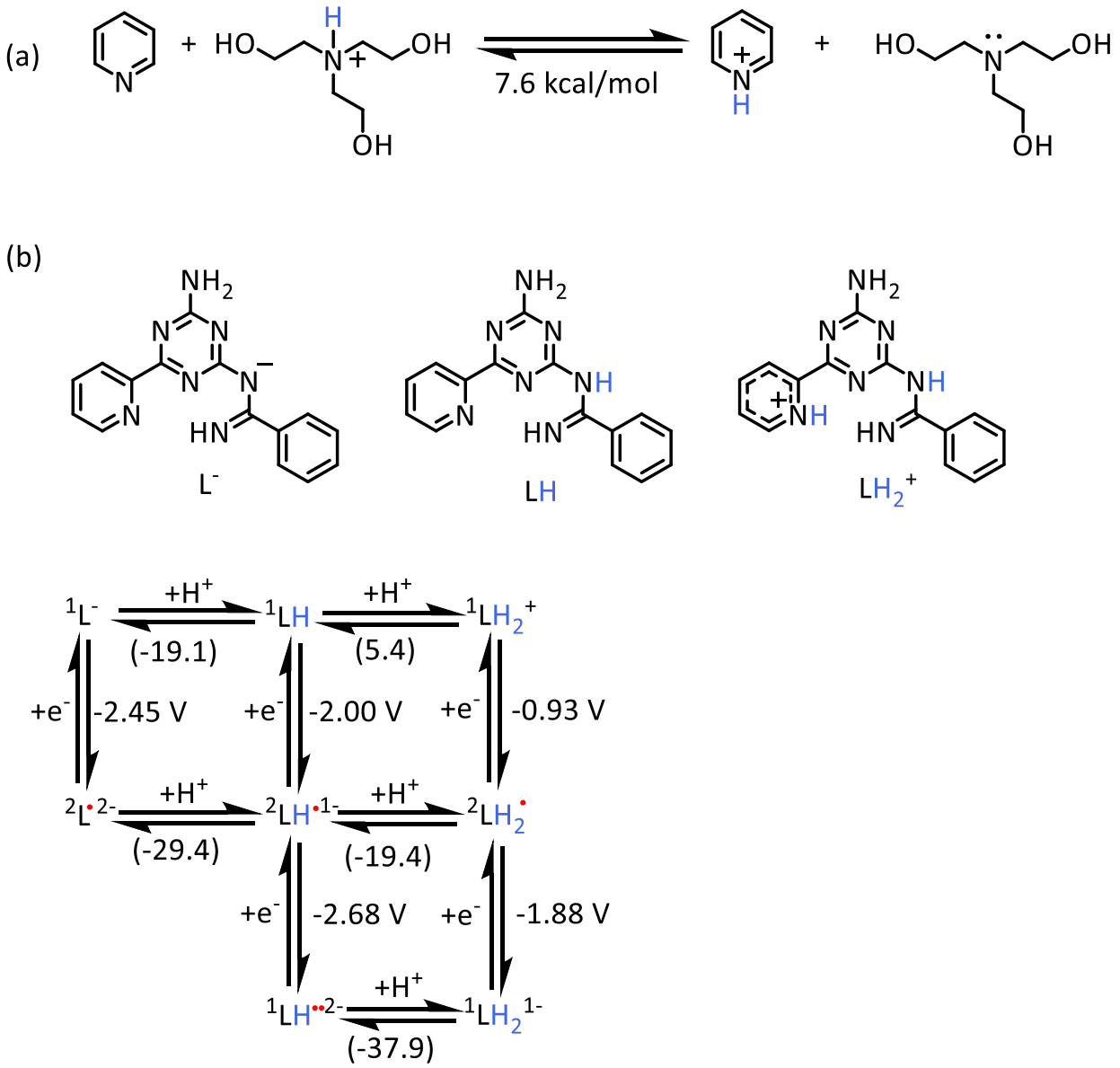

Scheme S1. (a) The calculated proton-transfer free energy from $[HTEOA]^+$ to pyridine in DMF solvent is shown on the horizontal arrow. (b) The calculated reduction potentials (E^0) and proton-transfer free energy of py-DAT-amidinate L^- in DMF solvent. The calculated reduction potentials E^0 vs. SCE (4.684 V) are shown on the vertical arrow. The calculated proton-transfer free energy from $[HTEOA]^+$ to the amidinate moiety of L^- and to the pyridine moiety of LH are shown on the horizontal arrow.

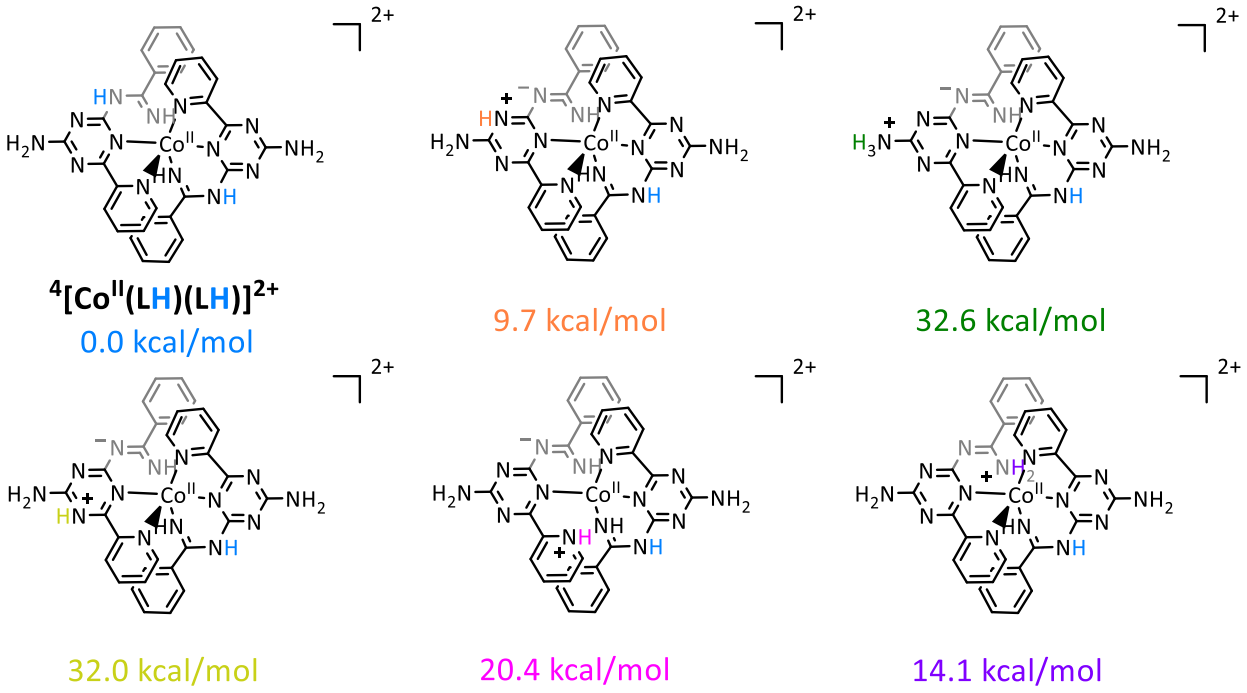

Scheme S2. Possible protonation states of ^{4}[Co^{II}(LH)(LH)]$^{2+}$. The free energies relative to the most stable protonation state are given in kcal/mol.

Table S4. The solvent corrected relative free energies for intermediates upon proton reductions of $^{1}[Co^{III}(L^{1-})(LH)]^{2+}$ (LH = py-DAT-amidine).

	Spin state	Broken Symmetry	E_{elec} (Hartree)	$<S^2>$	Absolute free energy (Hartree)	Relative free energy (kcal/mol)
$[Co^{II}(LH)(LH)]^{2+}$	S =1/2		-3308.099296	0.76	-3308.174994	8.7
	S = 3/2		**-3308.112934**	**3.76**	**-3308.188856**	**0.0**
$[Co^{II}(LH)(LH^{\bullet 1-})]^{1+}$	S = 0		-3308.224485	1.02	-3308.305239	5.9
	S = 1	BS(2,0)	-3308.225741	2.02	-3308.306446	5.2
	S = 1	**BS(3,1)**	**-3308.233384**	**2.99**	**-3308.314164**	**0.3**
	S = 2		**-3308.233672**	**6.02**	**-3308.314705**	**0.0**
$[Co^{II}(LH^{\bullet 1-})(LH^{\bullet 1-})]^{0}$	S = 1/2		-3308.337360	1.78	-3308.423593	7.4
	S = 3/2	BS(3,0)	-3308.338217	3.78	-3308.424683	6.7
	S = 3/2	**BS(4,1)**	**-3308.347807**	**4.77**	**-3308.434250**	**0.7**
	S = 5/2		**-3308.348793**	**8.78**	**-3308.435394**	**0.0**
$[Co^{II}(LH^{\bullet 1-})(LH_2^{\bullet})]^{1+}$	S = 1/2		-3308.780210	1.72	-3308.865919	3.7
	S = 3/2	BS(3,0)	-3308.779946	3.78	-3308.864958	4.3
	S = 3/2	**BS(4,1)**	**-3308.786604**	**4.45**	**-3308.871794**	**0.0**
	S = 5/2		-3308.780595	8.77	-3308.865886	3.7
$[Co^{II}(LH^{\bullet 1-})(LH_2^{1-})]^{0}$	S = 0		-3308.896201	1.01	-3308.985952	5.6
	S = 1		-3308.897148	2.02	-3308.986911	5.1
	S = 1	BS(3,1)	-3308.893628	3.26	-3308.976744	11.4
	S = 2	**BS(4,0)**	**-3308.905497**	**6.02**	**-3308.994971**	**0.0**
$[Co^{II}H(LH)(LH_2^{\bullet})]^{1+}$	S = 0		-3309.346058	1.02	-3309.430816	4.0
	S = 1	BS(2,0)	-3309.346952	2.02	-3309.431800	3.4
	S = 1	**BS(3,1)**	**-3309.352095**	**3.02**	**-3309.436764**	**0.3**
	S = 2		**-3309.352539**	**6.02**	**-3309.437248**	**0.0**
TS	S = 0		-3309.799434	1.01	-3309.399689	12.4
	S = 1		-3309.887846	2.01	-3309.401273	11.4
	S = 1	**BS(3,1)**	**-3309.899337**	**2.90**	**-3309.419385**	**0.0**
	S = 2		-3309.896370	6.02	-3309.414522	3.1
H_2	S = 0		-1.176714	0.00	-1.181206	

Table S5. The calculated relative free energies (ΔG), reduction potentials (E^0)[a], and proton-transfer free energy (ΔG^{PT})[b] for the Co intermediates in the most likely pathway for H_2 evolution (black paths in Scheme 6).

Reaction	ΔG (kcal/mol)	E˚ (V)	ΔG^{PT} (kcal/mol)
$[Ru(bpy)_3]^{2+} + e^- \rightarrow [Ru(bpy)_3]^{1+}$	-76.2	-1.38	-
$^1[Co^{III}(L^{1-})(LH)]^{2+} + e^- \rightarrow {}^2[Co^{II}(L^{1-})(LH)]^{1+}$	-106.2	-0.08	-
$^4[Co^{II}(L^{1-})(LH)]^{1+} + [HTEOA]^{1+} \rightarrow {}^4[Co^{II}(LH)(LH)]^{2+} + TEOA$	-	-	-3.1
$^4[Co^{II}(LH)(LH)]^{2+} + e^- \rightarrow {}^3[Co^{II}(LH)(LH^{\bullet 1-})]^{1+}$	-78.6	-1.27	-
$^3[Co^{II}(LH)(LH^{\bullet 1-})]^{1+} + e^- \rightarrow {}^4[Co^{II}(LH^{\bullet 1-})(LH^{\bullet 1-})]^{0}$	-75.4	-1.42	-
$^4[Co^{II}(LH^{\bullet 1-})(LH^{\bullet 1-})]^{0} + [HTEOA]^{1+} \rightarrow {}^4[Co^{II}(LH^{\bullet 1-})(LH_2^{\bullet})]^{1+} + TEOA$	-	-	3.6
$^3[Co^{II}(LH)(LH^{\bullet 1-})]^{1+} + e^- + H^+ \rightarrow {}^4[Co^{II}(LH^{\bullet 1-})(LH_2^{\bullet})]^{1+}$	-79.2[c]	-1.25	-
$^4[Co^{II}(LH^{\bullet 1-})(LH_2^{\bullet})]^{1+} + e^- \rightarrow {}^3[Co^{II}(LH^{\bullet -})(LH_2^{1-})]^{0}$	-77.3	-1.33	-
$^3[Co^{II}(LH^{\bullet -})(LH_2^{1-})]^{0} + [HTEOA]^{1+} \rightarrow {}^3[Co^{II}H(LH)(LH_2^{\bullet})]^{1+} + TEOA$	-	-	0.9
$^4[Co^{II}(LH^{\bullet 1-})(LH_2^{\bullet})]^{1+} + e^- + H^+ \rightarrow {}^3[Co^{II}H(LH)(LH_2^{\bullet})]^{1+}$	-83.8[c]	-1.05	-
$^3[Co^{II}H(LH)(LH_2^{\bullet})]^{1+} \rightarrow \mathbf{^3[TS_A]^{1+}}$	10.9	-	-
$^3[Co^{II}H(LH)(LH_2^{\bullet})]^{1+} \rightarrow {}^3[Co^{II}(LH)(LH^{\bullet 1-})]^{1+} + H_2$	-36.8	-	-

[a] E^o vs E^o(SCE) (4.684 V).[3, 4]

[b] ΔG^{PT} is the proton-transfer free energy from $[HTEOA]^+$ to the Co intermediate.

[c] Proton solvation free energy in DMF is -264.46 kcal/mol[17] and the proton free energy in the gas phase is obtained from Sackur–Tetrode equation (-6.28 kcal/mol).[18, 19]

Table S6. The calculated relative free energies (ΔG), reduction potentials (E^0)[a], and proton-transfer free energy (ΔG^{PT})[b] for other Co intermediates in the unlikely pathway for H_2 evolution.

Reaction	ΔG (kcal/mol)	E˚ (V)	ΔG^{PT} (kcal/mol)
$^1[Co^{III}(L^{1-})(LH)]^{2+} + [HTEOA]^{1+} \rightarrow {}^1[Co^{III}(LH)(LH)]^{3+} + TEOA$	-	-	9.5
$^1[Co^{III}(LH)(LH)]^{3+} + e^- \rightarrow {}^4[Co^{II}(LH)(LH)]^{2+}$	-125.4	0.75	-
$^4[Co^{II}(LH)(LH)]^{2+} + [HTEOA]^{1+} \rightarrow {}^4[Co^{II}(LH)(LH_2{}^{1+})]^{3+} + TEOA$	-	-	33.8
$^3[Co^{II}(LH)(LH^{\bullet 1-})]^{1+} + [HTEOA]^{1+} \rightarrow {}^3[Co^{II}(LH)(LH_2{}^{\bullet})]^{2+} + TEOA$	-	-	14.7
$^3[Co^{II}(LH)(LH_2{}^{\bullet})]^{2+} + e^- \rightarrow {}^4[Co^{II}(LH^{\bullet 1-})(LH_2{}^{\bullet})]^{1+}$	-86.5	-0.93	-
$^4[Co^{II}(LH^{\bullet 1-})(LH_2{}^{\bullet})]^{1+} + [HTEOA]^{1+} \rightarrow {}^4[Co^{II}H(LH)(LH_2{}^{1+})]^{2+} + TEOA$	-	-	9.8
$^4[Co^{II}H(LH)(LH_2{}^{1+})]^{2+} + e^- \rightarrow {}^3[Co^{II}H(LH)(LH_2{}^{\bullet})]^{1+}$	-86.2	-0.94	-

[a] E^o vs E^o(SCE) (4.684 V).[3, 4]

[b] ΔG^{PT} is the proton-transfer free energy from $[HTEOA]^+$ to the Co intermediate.

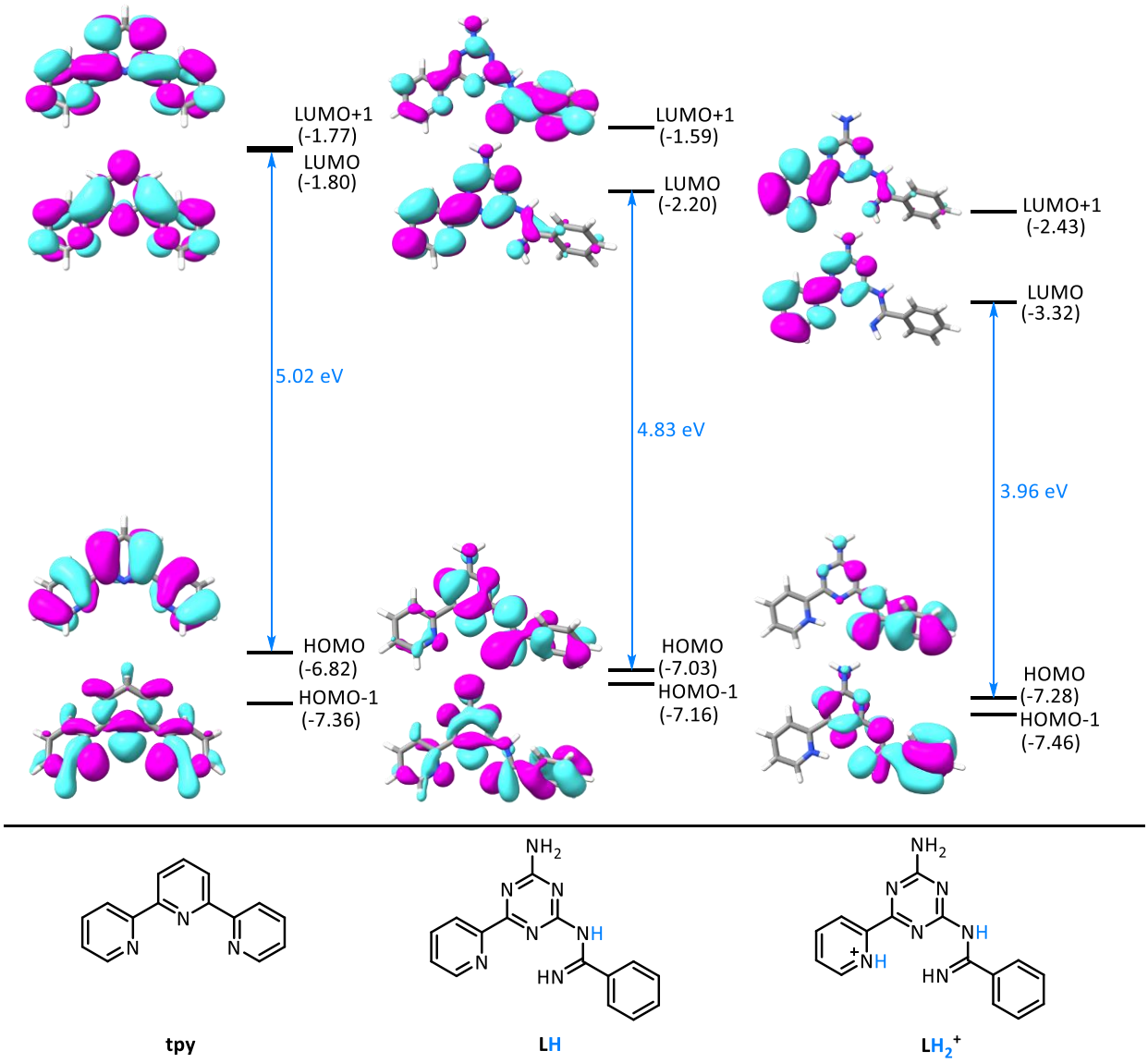

Fig. S9 Frontier molecular orbitals (MOs) and MO energies (in eV) of tpy (tpy = terpyridine), LH and LH_2^+ (LH = py-DAT-amidine).

Table S7. Calculated electronic excitation energies (eV) of tpy (tpy = terpyridine), LH and LH_2^+ (LH = py-DAT-amidine) from TD-DFT calculation.

		Electronic excitation energy (eV)	Oscillator strength (*f*)
tpy	**HOMO → LUMO (94.1%)**	**4.35**	0.43
	HOMO → LUMO+1 (88.6%)	4.63	0.22
LH	HOMO → LUMO (24.4%) HOMO-1 → LUMO (35.4%) HOMO-2 → LUMO (30.0%)	3.90	0.01
	HOMO → LUMO (50.1%) HOMO-2 → LUMO (31.6%)	**4.22**	0.08
LH_2^+	**HOMO → LUMO (75.2%)** HOMO-1 → LUMO (16.8%)	**3.47**	0.01
	HOMO → LUMO (21.2%) HOMO-1 → LUMO (48.5%) HOMO-2 → LUMO (14.3%)	3.52	0.01

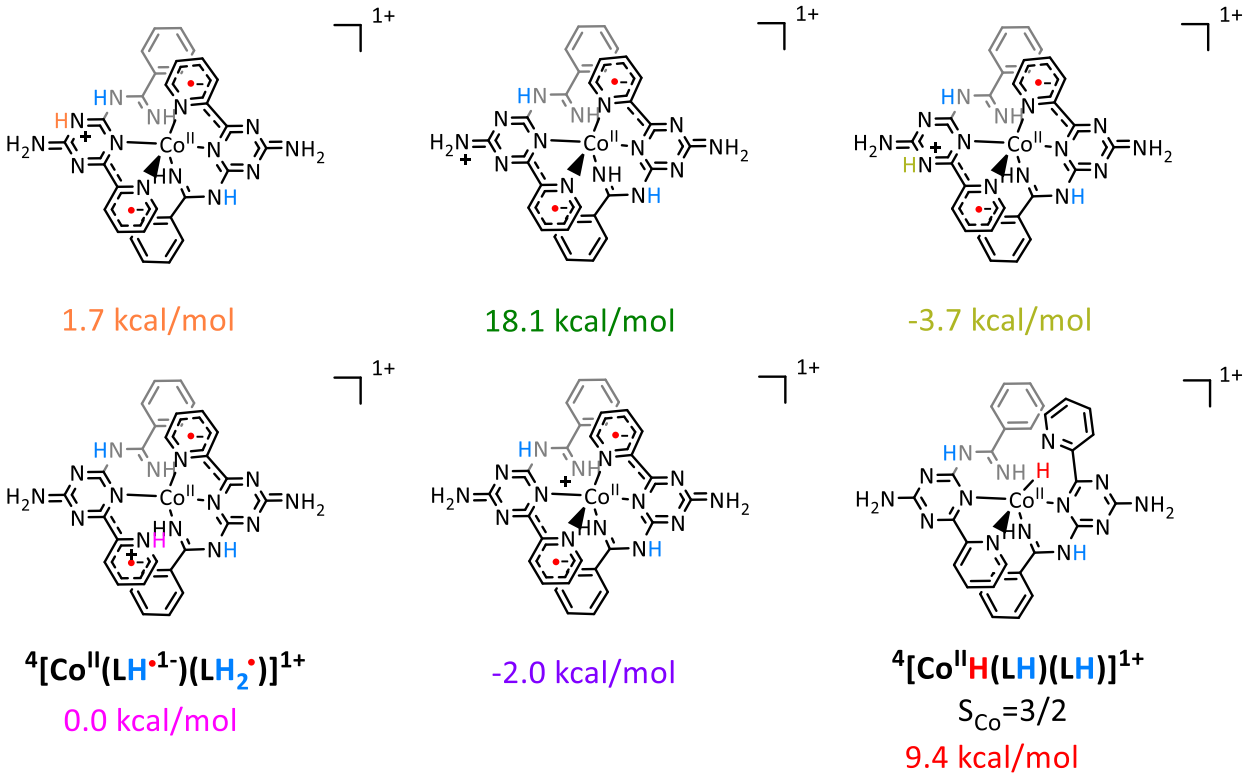

Scheme S3. Possible protonation states of $^4[Co^{II}(LH^{\bullet 1-})(LH_2^{\bullet})]^{1+}$. The relative free energies are given in kcal/mol.

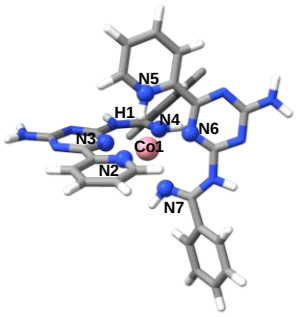

Co1-H1	**2.422**
Co1-N2	2.065
Co1-N3	2.086
Co1-N4	2.091
Co1-N5	3.163
Co1-N6	2.304
Co1-N7	2.045
N5-H1	1.017
N2-H1	2.103

$^{4}[Co^{II}(LH^{\bullet 1-})(LH_2^{\bullet})]^{1+}$

0.0

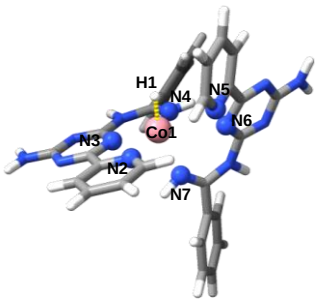

Co1-H1	**1.660**
Co1-N2	2.269
Co1-N3	2.142
Co1-N4	2.096
Co1-N5	4.002
Co1-N6	2.834
Co1-N7	2.140
N5-H1	3.319
N2-H1	2.759

$^{4}[Co^{II}H(LH)(LH)]^{1+}$

9.4

Fig. S10 The optimized geometries of $^{4}[Co^{II}(LH^{\bullet 1-})(LH_2^{\bullet})]^{1+}$ and $^{4}[Co^{II}H(LH)(LH)]^{1+}$. The relative free energies are shown in kcal/mol. The key bond distances are shown in Å.

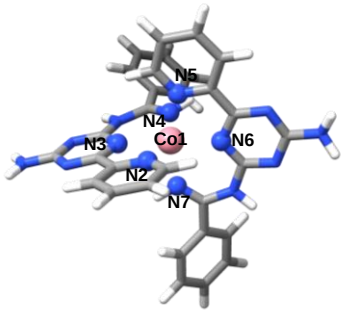

Co1-N2	2.208
Co1-N3	2.207
Co1-N4	2.128
Co1-N5	2.195
Co1-N6	2.091
Co1-N7	2.097

$^{3}[Co^{II}(LH)(LH^{\bullet 1-})]^{1+}$

0.0

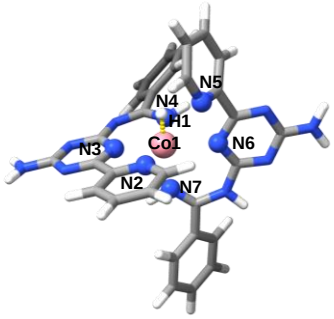

Co1-N2	2.076
Co1-N3	2.108
Co1-N4	1.953
Co1-N5	3.505
Co1-N6	2.271
Co1-N7	2.034
Co1-H1	1.473
N5-H1	2.533

$^{3}[Co^{III}H(L^{1-})(LH)]^{1+}$

39.8

Fig. S11 The optimized geometries of $^{3}[Co^{II}(LH)(LH^{\bullet 1-})]^{1+}$ and $^{3}[Co^{III}H(L^{1-})(LH)]^{1+}$. The relative free energies are shown in kcal/mol. The key bond distances are shown in Å.

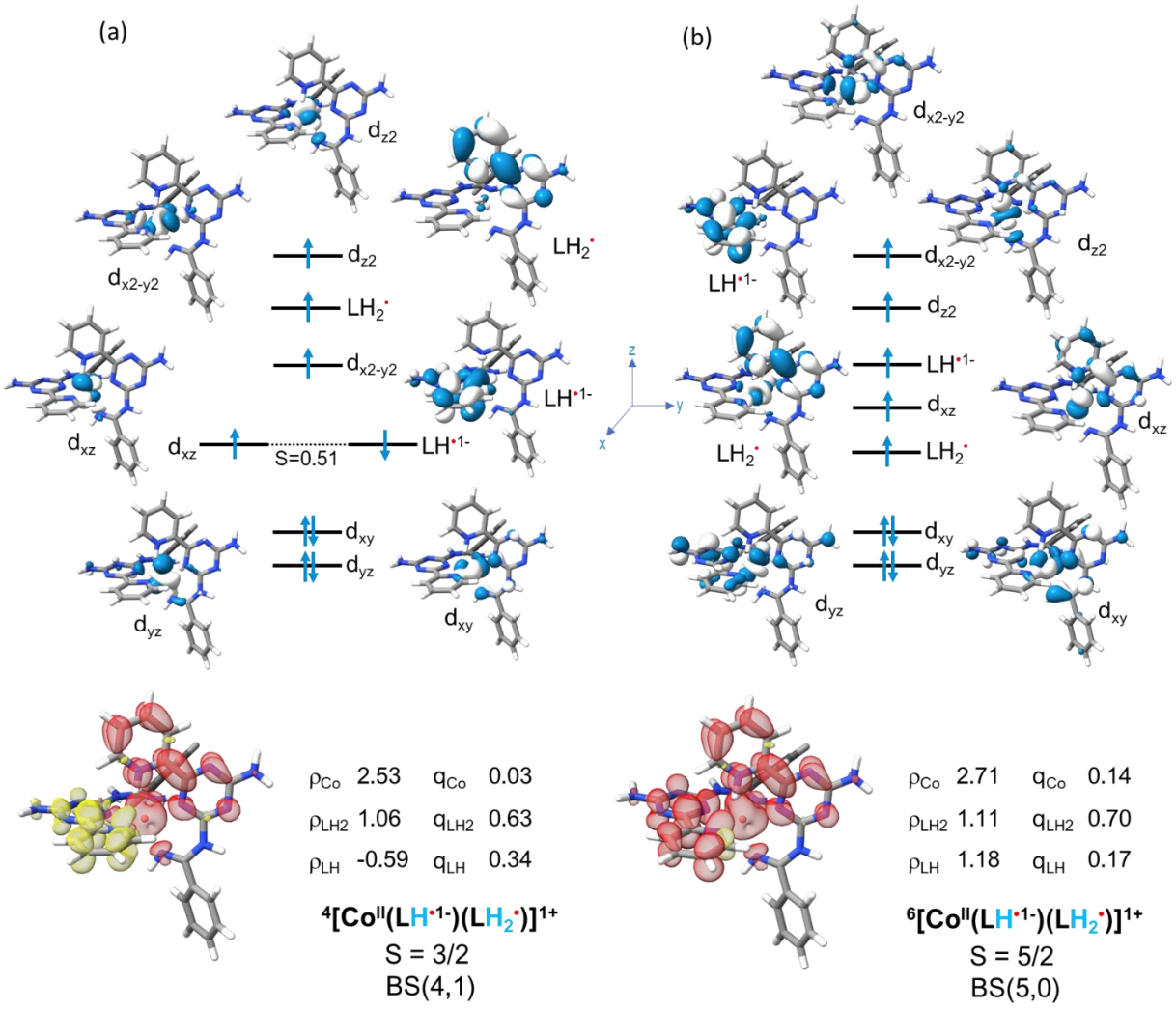

Fig. S12 (a) Frontier MOs and spin density plot of the $^4[Co^{II}(LH^{\bullet 1-})(LH_2^{\bullet})]^{1+}$ (S = 3/2, BS(4,1)). (b) Frontier MOs and spin density plot of the $^6[Co^{II}(LH^{\bullet 1-})(LH_2^{\bullet})]^{1+}$ (S = 5/2). The doubly occupied orbitals were represented by quasi-restricted orbitals and the singly occupied orbitals were represented by corresponding orbitals (isodensity = 0.05).

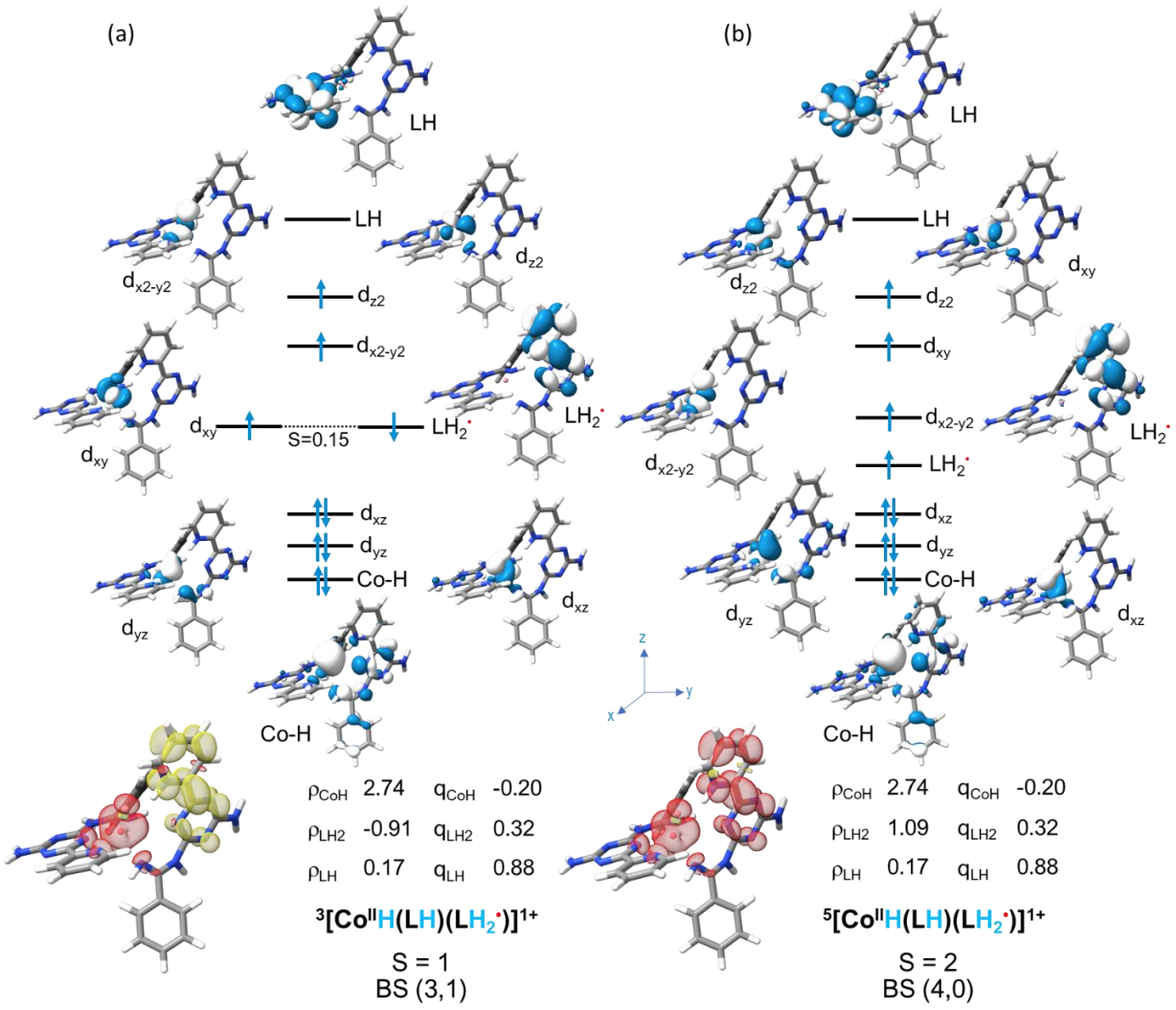

Fig. S13 (a) Frontier MOs and spin density plot of the $^3[Co^{II}H(LH)(LH_2^{\bullet})]^{1+}$ (S = 1, BS(3,1)). (b) Frontier MOs and spin density plot of the $^5[Co^{II}H(LH)(LH_2^{\bullet})]^{1+}$ (S = 2). The doubly occupied and unoccupied orbitals were represented by quasi-restricted orbitals and the singly occupied orbitals were represented by corresponding orbitals (isodensity = 0.05).

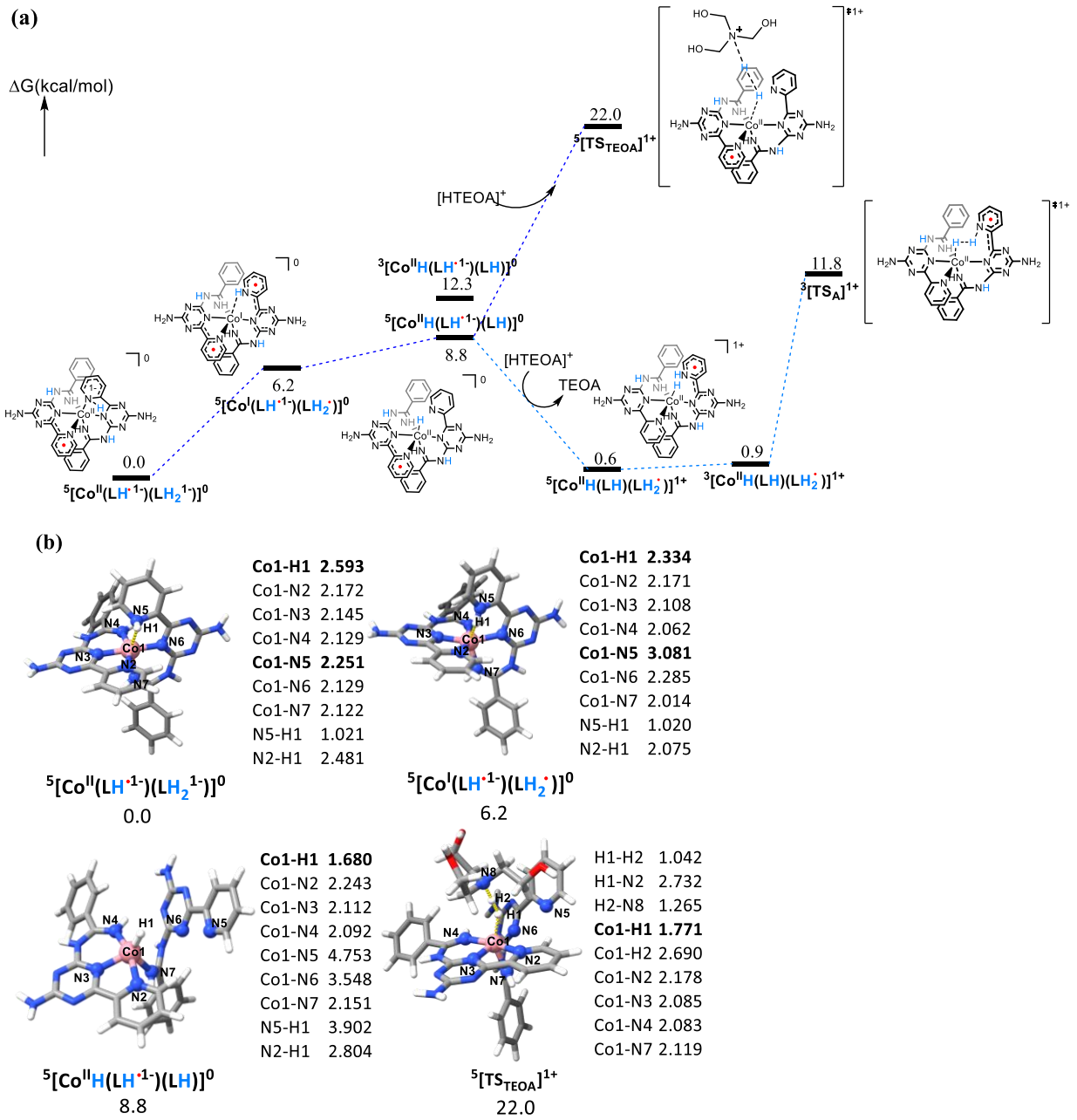

Fig. S14 (a) The relative free energy (in kcal/mol) for the H_2 elimination from the Co^{II}-H···HN(TEOA) vs. Co^{II}-H···HN(pyridine) intermediates. (b) Optimized geometries of $^5[Co^{II}(LH^{\bullet 1-})(LH_2^{1-})]^0$, $^5[Co^{II}H(LH^{\bullet 1-})(LH)]^0$ and $^5[\mathbf{TS_{TEOA}}]^{1+}$.

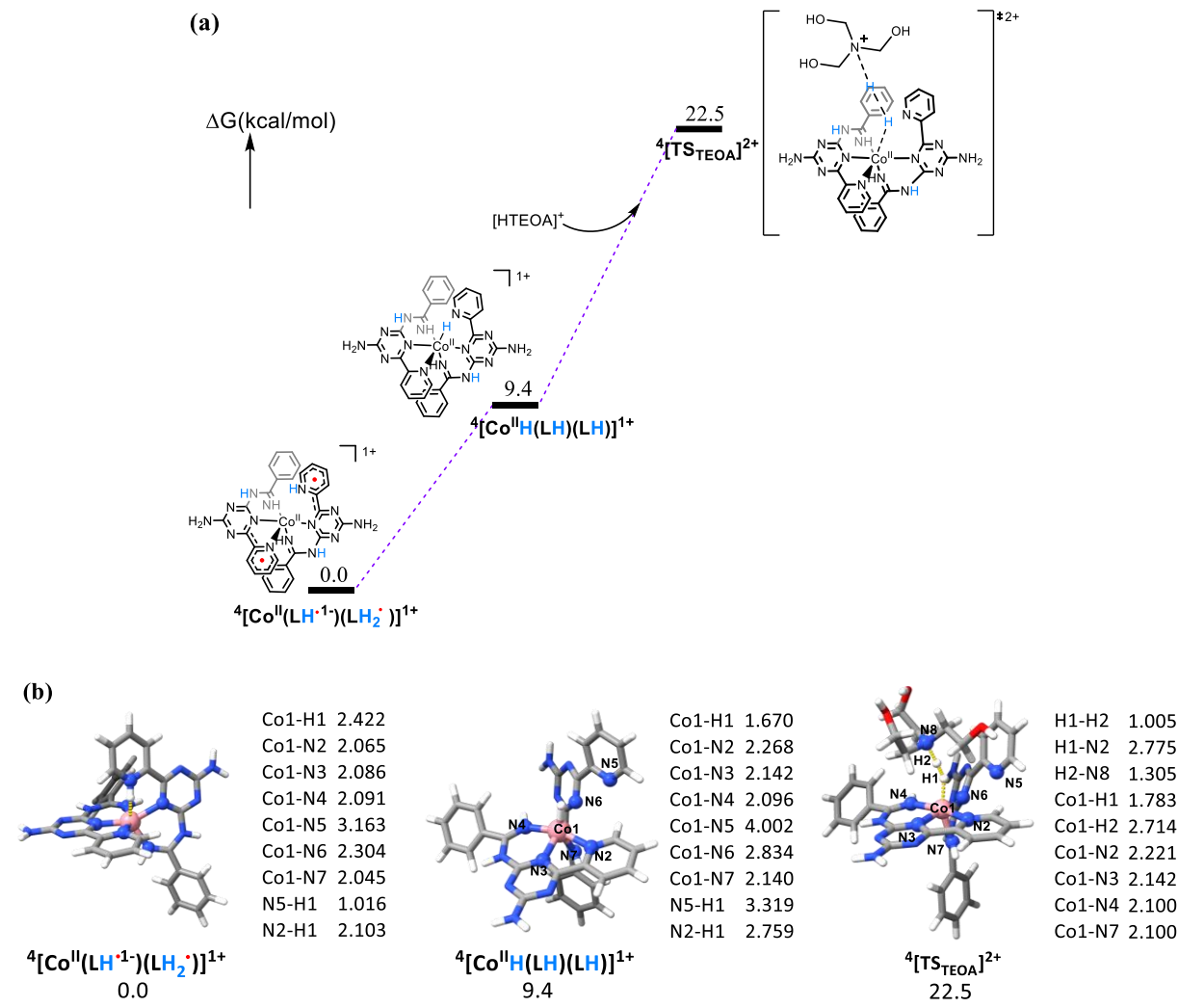

Fig. S15 (a) The relative free energy (in kcal/mol) for the H_2 elimination from the Co^{II}-H···HN(TEOA) intermediate. (b) Optimized geometries of $^4[Co^{II}(LH^{\bullet 1-})(LH_2^{\bullet})]^{1+}$, $^4[Co^{II}H(LH)(LH)]^{1+}$ and $^4[\mathbf{TS_{TEOA}}]^{2+}$.

References

1. C. J. Cramer, *Essentials of computational chemistry*, John Wiley & Sons, Chichester, England, 2 edn., 2004.
2. M. Namazian, C. Y. Lin and M. L. Coote, *Journal of Chemical Theory and Computation*, 2010, **6**, 2721-2725.
3. S. Trasatti, *Pure and Applied Chemistry*, 1986, **58**, 955-966.
4. V. V. Pavlishchuk and A. W. Addison, *Inorganica Chimica Acta*, 2000, **298**, 97-102.
5. H. Ferreira, M. M. Conradie and J. Conradie, *Data Brief*, 2019, **22**, 436-445.
6. S. Aroua, T. K. Todorova, P. Hommes, L. M. Chamoreau, H. U. Reissig, V. Mougel and M. Fontecave, *Inorg Chem*, 2017, **56**, 5930-5940.
7. W. F. Wacholtz, R. A. Auerbach and R. H. Schmehl, *Inorganic Chemistry*, 1986, **25**, 227-234.
8. S. Rajak, K. Chair, L. K. Rana, P. Kaur, T. Maris and A. Duong, *Inorg Chem*, 2020, **59**, 14910-14919.
9. L. Tong, L. Duan, A. Zhou and R. P. Thummel, *Coordination Chemistry Reviews*, 2020, **402**.
10. N. Queyriaux, R. T. Jane, J. Massin, V. Artero and M. Chavarot-Kerlidou, *Coordination Chemistry Reviews*, 2015, **304-305**, 3-19.
11. A. Rodenberg, M. Orazietti, B. Probst, C. Bachmann, R. Alberto, K. K. Baldridge and P. Hamm, *Inorganic Chemistry*, 2015, **54**, 646-657.
12. D. M. Arias-Rotondo and J. K. McCusker, *Chemical Society Reviews*, 2016, **45**, 5803-5820.
13. B. Probst, A. Rodenberg, M. Guttentag, P. Hamm and R. Alberto, *Inorganic Chemistry*, 2010, **49**, 6453-6460.
14. M. D. Karkas, O. Verho, E. V. Johnston and B. Akermark, *Chem Rev*, 2014, **114**, 11863-12001.
15. J. N. Harvey, M. Aschi, H. Schwarz and W. Koch, *Theoretical Chemistry Accounts*, 1998, **99**, 95-99.
16. J. Rodríguez-Guerra, *jaimergp/easymecp: v0.3.2 (v0.3.2). Zenodo. https://doi.org/10.5281/zenodo.4293422*, 2020.
17. Z. Marković, J. Tošović, D. Milenković and S. Marković, *Computational and Theoretical Chemistry*, 2016, **1077**, 11-17.
18. P. Surawatanawong, J. W. Tye, M. Y. Darensbourg and M. B. Hall, *Dalton Transactions*, 2010, **39**, 3093-3104.
19. G. J. Tawa, I. A. Topol, S. K. Burt, R. A. Caldwell and A. A. Rashin, *The Journal of Chemical Physics*, 1998, **109**, 4852-4863.